Pergamon

Journal of Structural Geology, Vol. 19, No. 10, pp. 1303 to 1321, 1997

PII: S0191-8141(97)00039-4
0191-8141/97 $17.00 + 0.00

Geometry of inverted faults and related folds in the Monterey Formation: implications for the structural evolution of the southern Santa Maria basin, California

GABRIEL GUTIÉRREZ-ALONSO

Departamento de Geología, Universidad de Salamanca, 37008 Salamanca, Spain

and

MICHAEL R. GROSS

Department of Geology, Florida International University, Miami, FL 33199, U.S.A.

(*Received* 7 *October* 1996; *accepted in revised form* 20 *April* 1997)

Abstract—A wide variety of mesoscopic structures observed in the Monterey Formation of coastal California reveal contrasting styles of deformation among mechanical units and provide a relative chronology of Neogene deformation for the southern Santa Maria basin. These structures, which include ptygmatically folded veins, folded beds of chert, inverted normal faults, fault-propagation folds and axial-planar breccia zones document an early extensional phase in the middle–late Miocene followed by two distinct episodes of contraction between the Pliocene and the present. Miocene normal faults in interbedded carbonates and mudstones were inverted, resulting in geometries that include normal faults truncated by bedding-plane detachments, low-angle thrusts and thrust duplexes, and normal faults reactivated in reverse. Fault-block geometry, drag folds and culmination folds are characteristic features that help identify inverted structures. Normal fault inversion coincides with the development of early chert folds and related structures higher in the stratigraphic section, representing a regional phase of layer-parallel contraction. The second phase of regional contraction resulted in the development of a fold-and-thrust belt, which in the Monterey Formation is manifested by detachment and fault-related folds aligned parallel to regional fold axes. Effects of silica diagenesis contribute to the development of mesoscale structures throughout the deformation history of the Monterey Formation. © 1997 Elsevier Science Ltd.

INTRODUCTION

Inversion tectonics refer to the large-scale reactivation of pre-existing normal faults in a reverse sense due to a change in tectonic regime from extension to compression. The control pre-existing extensional structures exert on the style of subsequent compressional deformation has been recognized in many orogenic belts such as the Alps (e.g. Argand, 1911; Glennie and Boegner, 1981; Ziegler, 1983; Bally, 1984; Butler, 1989), the Variscan belt (Martínez-Catalán *et al.*, 1992), the Zagros (Jackson, 1980), the Canadian Rockies (McClay *et al.*, 1989), the Andes (Grier *et al.*, 1992) and along the California borderland (Namson and Davis, 1990; Crouch and Suppe, 1993). Most examples cited in the literature describe the deformation of graben- or half-graben-shaped basins filled with syn-rift sediments (e.g. Cartwright, 1989; Chapman, 1989; Mitra, 1993; Buchanan and Buchanan, 1995). Reactivation of these basin-scale normal faults is commonly followed by out of sequence thrusting (Hayward and Graham, 1989; McClay, 1989; Williams *et al.*, 1989).

Butler (1989) reported geometries on a regional scale for the Frontal Pennine thrust in the Alps where shortening is accommodated by bedding-parallel slip and low-angle thrusting, resulting in the transection of normal faults rather than their reactivation upon inversion. Analogous normal fault 'decapitation' is reported by Mitra (1993) as a possible feature, although no field cases or experimental models of this kind are presented. Because the mechanism for accommodating shortening depends upon rheology, strain partitioning occurs as competent units deform by thrusting and bed-parallel slip, while incompetent layers deform through homogeneous layer-parallel shortening.

This paper discusses the geometries and origin of outcrop-scale inverted faults in the Miocene Monterey Formation exposed along the Santa Maria coastline of California. The Monterey Formation exhibits a wide range of rheologies, such that deformation style varies among mechanical units; contraction in mudstones may be accommodated by fault inversion, while simultaneous folding may occur in siliceous beds. In order to help constrain the Neogene tectonic evolution of the southern Santa Maria basin, we construct a chronology of deformation based on mesoscale folds and inverted faults preserved in the Monterey Formation. Owing to the profound effects of silica diagenesis on rock mechanical properties, we also discuss the interaction between diagenesis and the development of structures in the Monterey Formation.

TECTONIC SETTING

Structural trends in the Coast Ranges of California are dominated by the NW–SE-trending San Andreas transform system, including large regional faults such as the

San Andreas, Rinconada, Nacimiento and Hosgri faults, as well as the smaller Huasna, Little Pine, Santa Maria, Orcutt and Lions Head faults (Fig. 1) (Jennings, 1977; Namson and Davis, 1990).

The triangular-shaped onshore Santa Maria basin, located in the southern Coast Ranges of central California, is bounded by the Hosgri fault to the west, the western Transverse Ranges to the south, and the Nacimiento–Rinconada fault to the east and north (Fig. 1). The formation and subsequent deformation of the basin are closely related to the Cenozoic tectonic development of the California borderland. The Santa Maria basin is one of a series of basins that formed along the California borderland in response to the onset of regional transtension at approximately 23 Ma ago at the Oligocene–Miocene boundary (Howell *et al.*, 1980; Vedder, 1987). The basin may have formed either as a pull-apart structure within a wrench system (Hall, 1981; McCulloch, 1989) or, alternatively, as a result of pure extension along a detachment above a metamorphic core complex (Crouch and Suppe, 1993). Structures reflecting Miocene extension within the Santa Maria basin include high-angle normal faults and growth faults mapped on offshore seismic lines (Crain *et al.*, 1985; McCulloch, 1989) and faults predicted from onshore well control (Namson and Davis, 1990), as well as syn-compactional normal faults observed in outcrops along the coastline (Gross, 1995). A switch to regional transpression took place in the Pliocene, perhaps initiated by the clockwise rotation of the Pacific plate at ~3–4 Ma (Cox and Engebretson, 1985; Harbert and Cox, 1989), and is manifested by the termination of growth faulting and the development of the Santa Maria fold-and-thrust belt (Crouch *et al.*, 1984; McCulloch, 1989; Namson and Davis, 1990; Clark *et al.*, 1991; Nicholson *et al.*, 1992). Consequently, numerous large faults that originally served as extensional growth faults during the Miocene were subsequently inverted into thrust geometries during the course of the past 3–5 Ma (Namson and Davis, 1990; McIntosh *et al.*, 1991; Nicholson *et al.*, 1992). Geological and paleomagnetic studies reveal the western Tranverse Ranges, located immediately south of the onshore Santa Maria basin, have undergone ~90° clockwise rotation since the middle Miocene (e.g. Crouch, 1979; Luyendyk *et al.*, 1980; Hornafius, 1985).

LOCAL GEOLOGY

The structural grain in the southern onshore Santa Maria basin is dominated by a series of E–W-trending folds (Woodring and Bramlette, 1950; Jennings, 1977; Dibblee, 1988c), which are manifestations of a S-directed, actively developing, fold-and-thrust belt. Namson and Davis (1990) interpret the anticlinal trends as fault-bend and fault-propagation folds that form above ramps emanating from a regional detachment situated at a depth of 11–14 km. The major anticlinal trend in the southern Santa Maria basin is the ~100°-trending Lompoc–Purisima anticline (LPA), which extends more than 45 km eastward from the Pacific coastline (Fig. 1). Balanced cross-sections drawn from well data reveal an asymmetric fold with a steeper north limb, hence the LPA is considered a fault-bend fold developing above a N-verging backthrust, which splays from the main detachment beneath the Santa Rita Valley (Namson and Davis, 1990). The Lompoc–Purisima anticline is flanked to the south by the synclinal trough of the Santa Rita Valley, and to the north by the San Antonio–Los Alamos syncline. The northernmost structure belonging to the series of E–W-oriented folds is the Casmalia–Orcutt anticlinal trend. The Lions Head fault intersects the coastline along the continuation of this trend, juxtaposing Jurassic Point Sal ophiolite to the north against the lower Monterey Formation.

THE MONTEREY FORMATION

The Monterey Formation was deposited in a series of deep marginal basins along the California borderland between 17 and 5.5 Ma, and consists of a wide variety of lithological units including dolostone, limestone, siliceous and carbonaceous shale, mudstone, diatomite, opal-CT and quartz porcellanite and chert, and laminated organic-phosphatic marlstone (e.g. Bramlette, 1946; Pisciotto and Garrison, 1981; Isaacs, 1982; Compton, 1991). In the Santa Maria basin the Monterey Formation can reach thicknesses up to 1150 m, and is divided by MacKinnon (1989) into four informal members (Fig. 2). Bed thicknesses typically fall within a range of 5–100 cm, resulting in a heterogeneous thin–medium bedded rock mass where style of deformation is a function of mechanical stratigraphy.

For example, Narr and Suppe (1991) divide the Monterey Formation into a series of 'jointing' and 'non-jointing' beds. In addition, fracture partitioning occurs in the phosphatic member (the carbonaceous marl member of Isaacs, 1983), whereby opening mode veins developed in limestone units and normal faults propagated in mudstone units in response to the same tectonic stresses (Gross, 1995). Thin carbonate and siliceous beds within mudstone mechanical units of the phosphatic member are offset across these normal faults, serving as excellent marker horizons for measuring displacement and extension (Gross and Engelder, 1995; Gross *et al.*, 1997). While brittle failure predominates in porcellanites and carbonates, detachment folds develop in the pure siliceous cherts of the upper calcareous–siliceous member (e.g. Grivetti, 1982; Dunham and Blake, 1987; MacKinnon, 1989; Behl and Garrison, 1994). Thus, mechanical behavior of the Monterey Formation under applied tectonic forces depends to a large extent upon lithology.

Silica in the Monterey Formation originated as diatom frustules in the form of amorphous opal-A (Bramlette, 1946; Jones and Segnit, 1971). Because opal-A is unstable

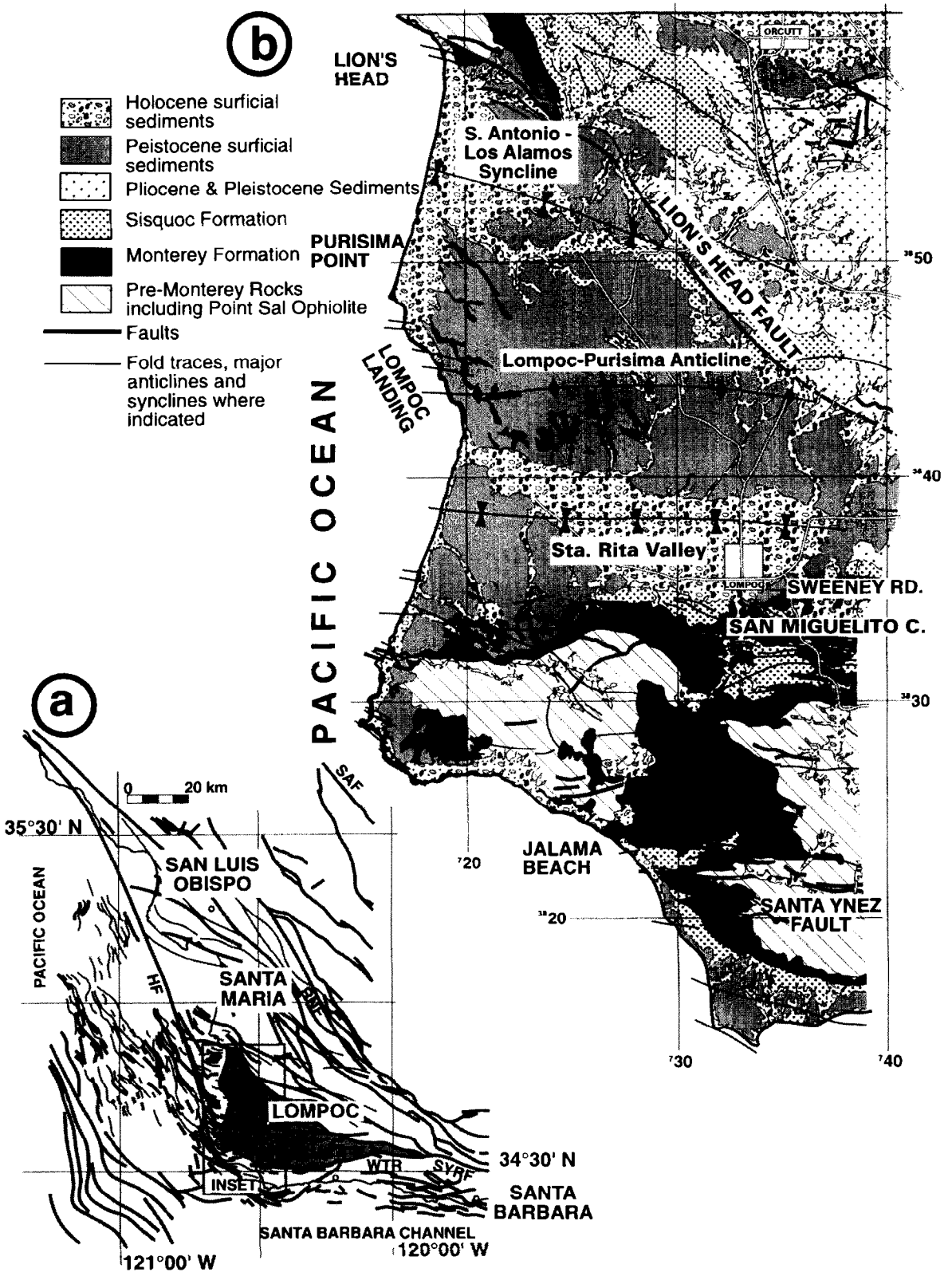

Fig. 1. (a) Regional tectonic map of the western Transverse Ranges and southern Coast Ranges compiled from Jennings, 1977; Sylvester and Darrow, 1979; McCulloch, 1989; Namson and Davis, 1990; Nicholson *et al.*, 1992; Cummings and Johnson, 1994; Steritz and Luyendyk, 1994; and Vittori *et al.*, 1994. NRF, Nacimiento–Rinconada fault; HF, Hosgri fault; SAF, San Andreas fault; SSMB, southern Santa Maria basin; SYRF, Santa Ynez River fault; WTR, western Transverse Ranges. Solid lines, faults; dashed lines, fold-axial traces. (b) Geological map of the southern Santa Maria basin compiled from Dibblee (1988a,b,c, 1989a,b) and Namson and Davis (1990). Stations for detailed structural analysis are Lions Head, Purisima Point, Lompoc Landing, Jalama Beach, San Miguelito Canyon and Sweeney Road. Thin solid lines, main roads.

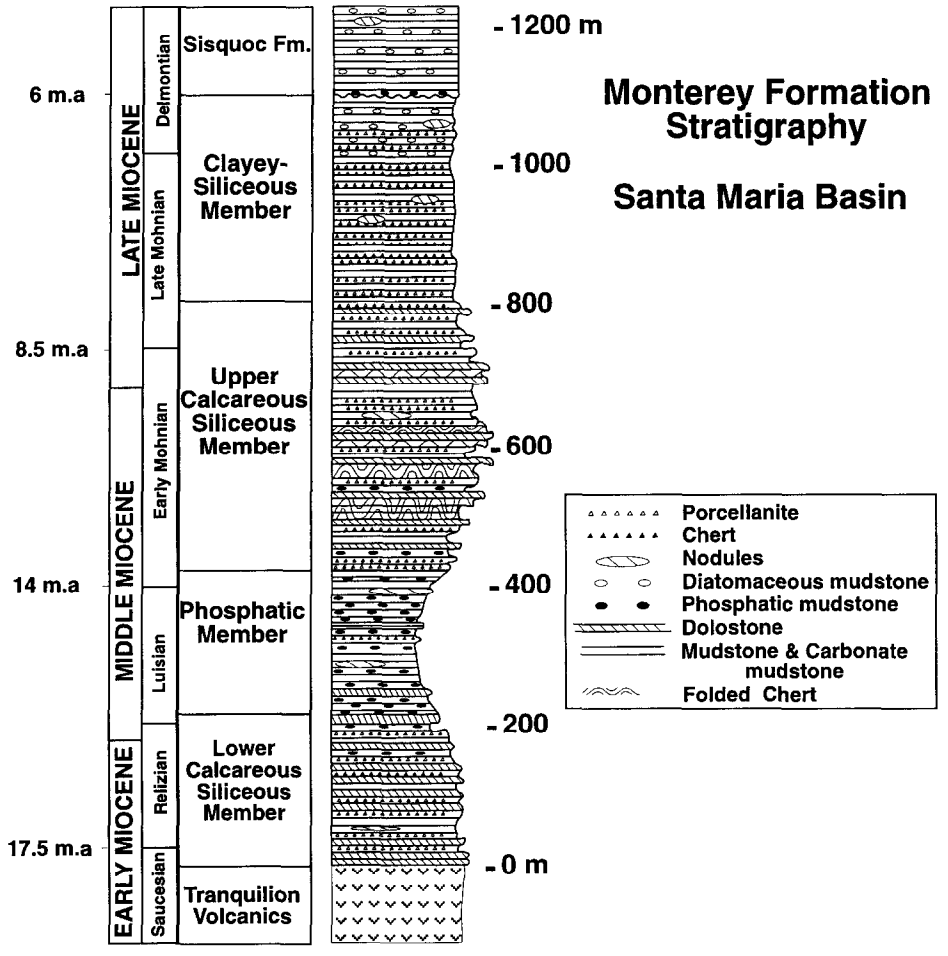

Fig. 2. Stratigraphic column of the Monterey Formation in the Santa Maria basin (after MacKinnon, 1989).

over geological time spans, the combined effects of time and burial eventually transform the biogenic silica to quartz (Murata and Larson, 1975; Isaacs, 1982). The diagenetic process consists of two separate dissolution–precipitation phases. Under increasing burial depth and temperature, opal-A converts to metastable opal-CT. Further increases in temperature result in the dissolution of opal-CT and the reprecipitation of the silica phase as quartz. In addition to burial temperature, timing of silica diagenesis is also a function of silica purity, such that at a given locality adjacent beds can be at different stages of silica diagenesis depending upon bulk composition (Isaacs, 1982; Behl and Garrison, 1994).

A significant amount of silica is added to cherts during diagenesis, often resulting in a net volume increase and thickening of individual chert beds (Steinitz, 1981; Behl and Garrison, 1994). For the Monterey Formation, Behl and Garrison (1994) estimate that 2–4 times the original amount of silica in the form of pore-filling cement was added to that already present in opal-A beds to form opal-CT chert. An additional 5–40% silica by volume was added during opal-CT chertification as cement filling within extension fractures, breccias and between boudins. The transformation from opal-CT to quartz also resulted in additions of silica, perhaps up to 10 times as suggested by data of Behl and Garrison (1994). Much of the silica that precipitated during early diagenesis served to reduce porosity by filling pore spaces. However, contorted (intensely folded) and brecciated chert beds record a net dilation (i.e. volume-increase thickening) due to the precipitation of silica-rich fluids in between fractured and rotated blocks of bedded chert (Behl and Garrison, 1994). In all likelihood the source of additional silica for chert beds was provided by interbedded porcellanites and siliceous mudstones, which exhibit compactional and tectonically induced pressure solution features such as bed-parallel stylolites and high-angle clay seams (e.g. Pisciotto, 1978; Snyder *et al.*, 1983).

LOCALITIES AND CROSS-SECTIONS

Structural data were collected from the Monterey Formation at Lions Head, Purisima Point, Lompoc Landing, Sweeney Road, San Miguelito Canyon and Jalama Beach (Fig. 1). Schematic cross-sections along with stereoplots are presented in Figs 3–6. Outcrops along Sweeney Road and San Miguelito Canyon are located near the southern margin of the basin, where regional folds display relatively tight wavelengths of

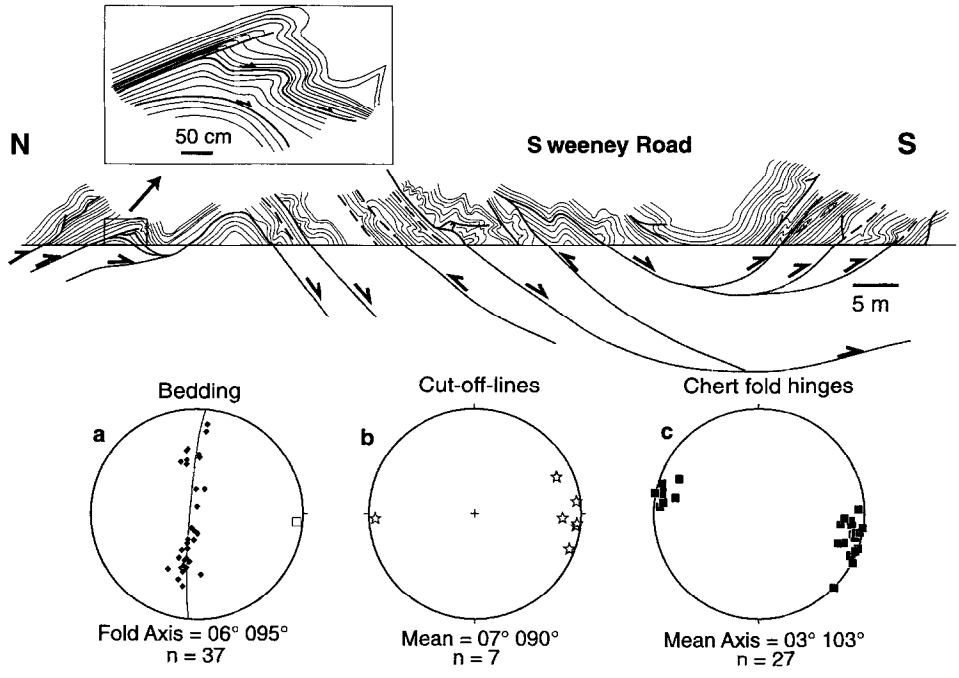

Fig. 3. Sketch of Sweeney Road cross-section along with structural data. Stereoplots represent: (a) π-diagram, the white square is the calculated regional fold axis; (b) thrust cutoff lines indicating a N–S transport direction for the thrusts; and (c) Group III fold hinges. Note consistent alignment of cutoff lines and chert fold hinges to the regional fold axis. Arrows pointing to the north are related to backthrusts.

~30–50 m. Outcrop-scale structures in the laminated cherts and porcellanites of the clayey siliceous member include detachment folds and fault-propagation folds with a S-directed vergence. Folds observed on the surface appear to have formed as a result of blind thrusts splaying off detachment horizons at depth, and bedding-plane detachments themselves are folded progressively during deformation (Figs 3 & 4). Poles to bedding plotted in π-diagrams reveal cylindrically shaped, horizontal to gently plunging E–W-trending regional folds with axes of 06°/095° (plunge°/trend°) and 14°/099° for Sweeney Road (Fig. 3) and San Miguelito Canyon (Fig. 4), respectively. Lompoc Landing and Purisima Point (Fig. 5) are part of a continuous coastal exposure of the upper calcareous–siliceous member along the broad crest and limbs of the Purisima

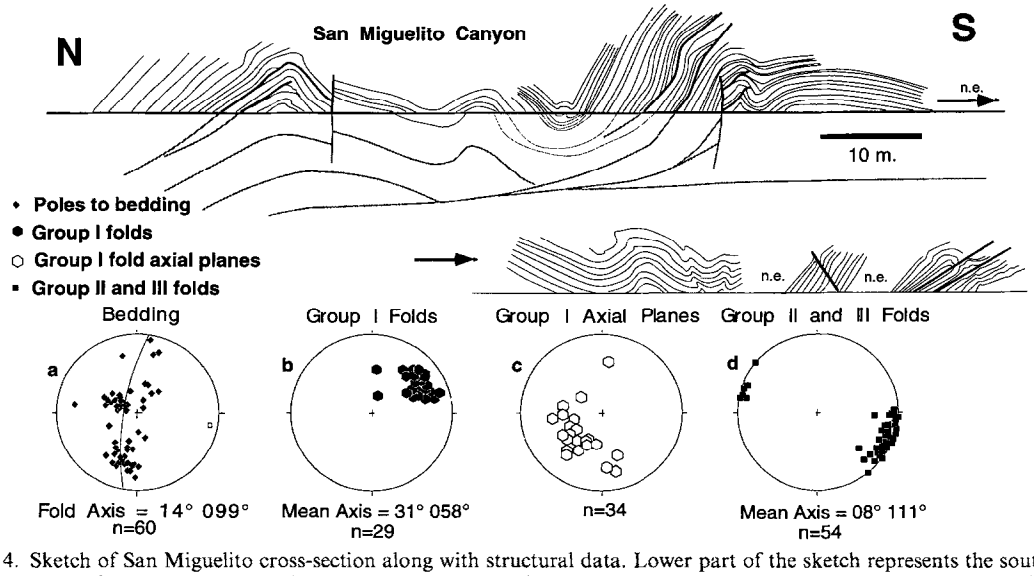

Fig. 4. Sketch of San Miguelito cross-section along with structural data. Lower part of the sketch represents the southern continuation of the upper part, and 'ne' means 'not exposed'. Stereoplots represent: (a) π-diagram, white square is the calculated regional fold axis; (b) Group I fold hinges; (c) poles to axial planes of Group I folds; and (d) hinges of Groups II and III folds.

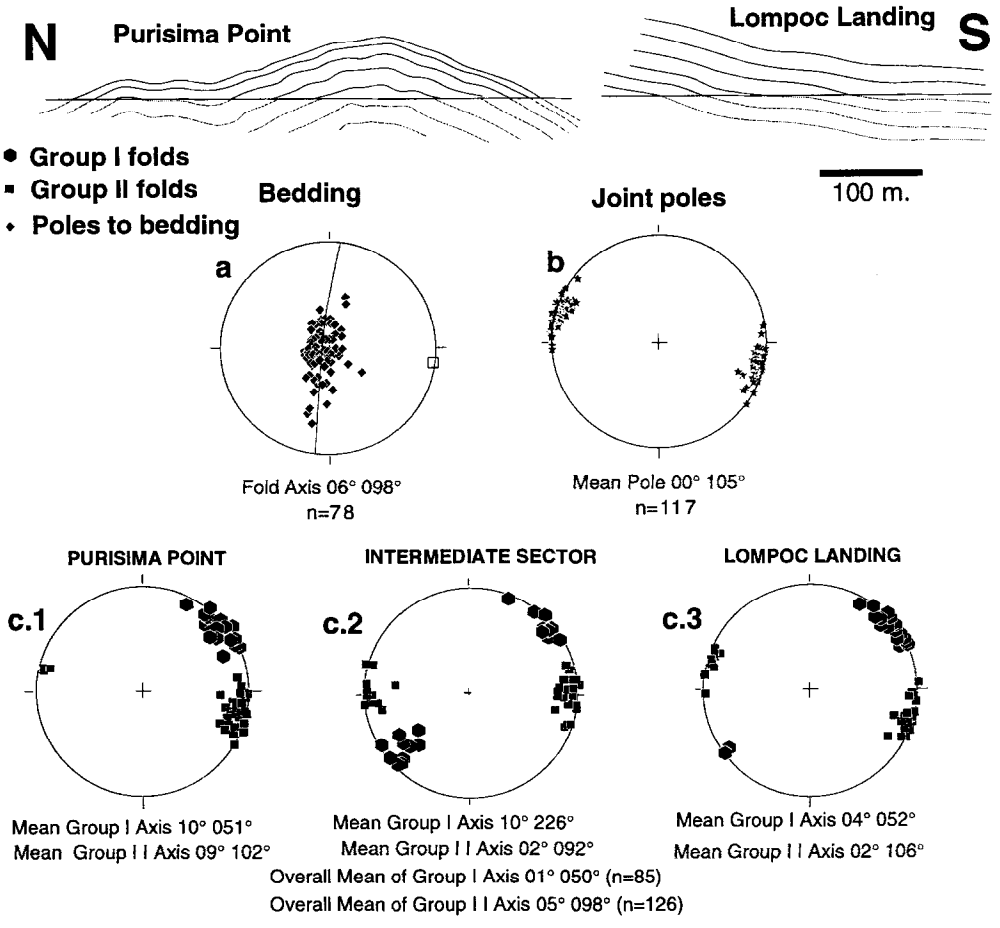

Fig. 5. Sketch of Purisima Point–Lompoc Landing cross-section with structural data. Stereoplots depict: (a) π-diagram, white square is the calculated regional fold axis; (b) poles of systematic joints normal to Group II fold hinges; and (c) fold hinges of Groups I and II folds in different locations along the coastline (c1, c2 and c3).

anticline. Bedding ranges from horizontal to moderately dipping, resulting in minimal structural relief. A regional fold axis of 06°/098° is derived by combining bedding attitudes from Lompoc Landing and Purisima Point (Fig. 5). Moderate to vertically dipping beds at Lions Head (Fig. 6) expose nearly complete sections of the phosphatic and upper calcareous–siliceous members of the Monterey Formation. The base of the section begins to the north with slightly overturned and dragged beds in contact with the Lions Head fault (Fig. 6), and the youngest beds are exposed in a syncline approximately 500 m further south along the coastline. Here the regional fold axis derived from poles to bedding is 19°/286° (Fig. 6a). The anomalous non-horizontal regional axis may be related to movement along the Lions Head fault.

GEOMETRY OF INVERTED NORMAL FAULTS

The earliest deformation recorded in the Monterey Formation along the Santa Maria coastline is a phase of extension interpreted as Miocene in age (Gross, 1995), confirmed by normal fault data presented in Fig. 6(a–c). Fracture partitioning resulted in the development of these normal faults in mudstones (mechanical units dominantly comprising organic-rich marlstone interbedded with thin carbonates) and the coeval propagation of opening mode veins and joints in carbonates and siliceous units (Fig. 7a) (Gross, 1995). The lack of sedimentary thickening in the hangingwall indicates these normal faults did not grow during sedimentation. However, bedding-normal ptygmatic folding and thrusting of veins along with passive rotation of faults in mudstones indicate these structures formed prior to or during compaction. These early normal faults in the mudstone mechanical units were subsequently inverted.

Description of inversion-related structures

Inversion-related structures were observed in the phosphatic member from Jalama beach to Lions Head along the Santa Maria coastline, with Lions Head providing the best examples due to exposure of vertical beds in the intertidal zone. A typical example of inverted faults in the Monterey Formation is illustrated in Fig. 8, which depicts offsets of limestone beds within a laminated organic-rich phosphatic mudstone.

Extension of bedding along high-angle conjugate

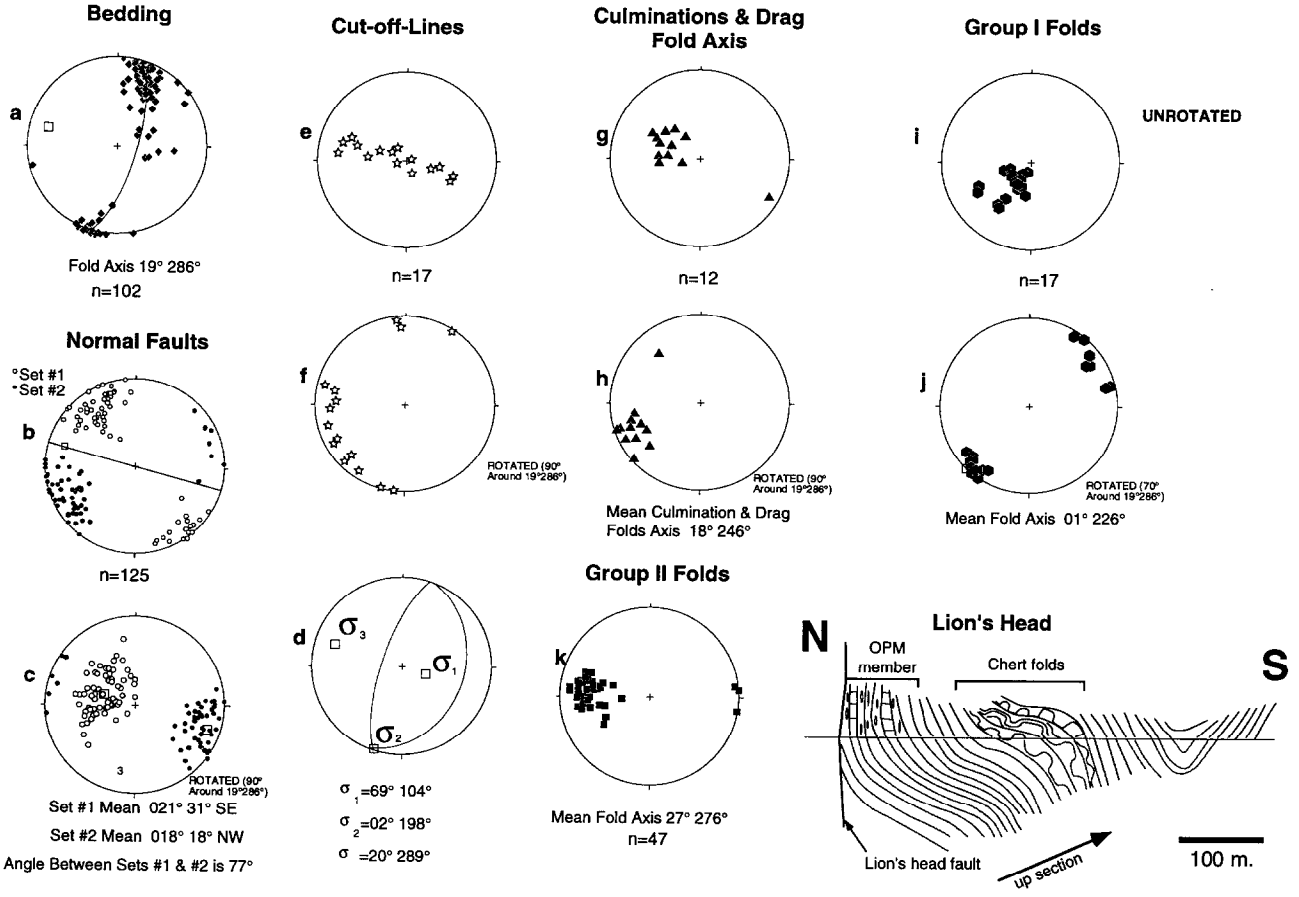

Fig. 6. Sketch of Lion's Head cross-section with structural data. Stereoplots show: (a) π-diagram, white square is the calculated fold axis; (b) poles of normal faults separated into two conjugate populations; (c) normal fault orientations after restoring bedding to its original position by 90° rotation around 19°/286°; (d) principal stress orientations inferred from conjugate fault populations; (e) orientation of cutoff lines of inverted faults; (f) orientation of cutoff lines of inverted faults rotated; (g) culminations and drag folds related to the inverted faults; (h) culminations and drag folds related to the inverted faults rotated; (i) Group I fold hinges; (j) Group I fold hinges rotated; and (k) Group II fold hinges.

normal faults is apparent, resulting in graben and half-graben structures. However, thrust displacement and duplication of pre-existing normal faults in area 'x' indicate a later phase of shortening. One key observation that points to inversion is the geometry of block-bounding fault surfaces. Note the dip direction of block walls (dashed lines) in area 'z' is opposite to the expected geometry for a simple thrust as depicted in Fig. 8(b). Also note that, in order to restore the upper limestone bed to its original unfaulted condition, a component of contractional bedding-plane slip must be removed. Normal fault offsets in Fig. 8(a) reveal two styles of inversion: in the lower-left portion of Fig. 8(a), a pre-existing S-dipping normal fault is reactivated in reverse, while in the upper-right the normal fault is truncated and offset by slip along the bed boundary. In the absence of syn-rift sedimentation, proof of inversion through purely reactivated normal faults may not be apparent. When inversion is partially accommodated by bedding-plane slip and low-angle thrusting, however, evidence for the initial phase of extension remains preserved (Fig. 8c).

At Lions Head the inversion-related structures, associated with 5–30 cm thick limestone and dolostone beds within organic-rich marlstone units, are characterized by: (1) truncation of normal faults by bedding-plane slip with senses of transport both to the east and west; (2) low-angle thrusts with hangingwall and footwall deformation (e.g. Ramsay, 1992); (3) thrusting along pre-existing normal fault planes (i.e. the reactivation of normal faults in reverse); and (4) thrust duplexes. Drag folds and culmination folds (fault-bend folds) are commonly associated with bedding-plane slip and low-angle thrusting, respectively. These inversion-related deformation features are found in combination with one another with various degrees of structural complexity.

A series of photographs and sketches of inversion-related structures are presented in Figs 7(b) & 9(a–g). Figure 9(a) shows a drag fold that developed in the footwall during contraction accommodated by bedding-plane slip. The carbonate bed, originally offset by a normal fault, is presently thrust-duplicated. In addition, folding results in the passive rotation of the pre-existing normal fault bounding the footwall block. Similar drag folds that formed in conjunction with bedding-plane slip are seen in Fig. 9(b & d). Note the opposite sense of motion along two bedding-plane slip zones in Fig. 9(d)

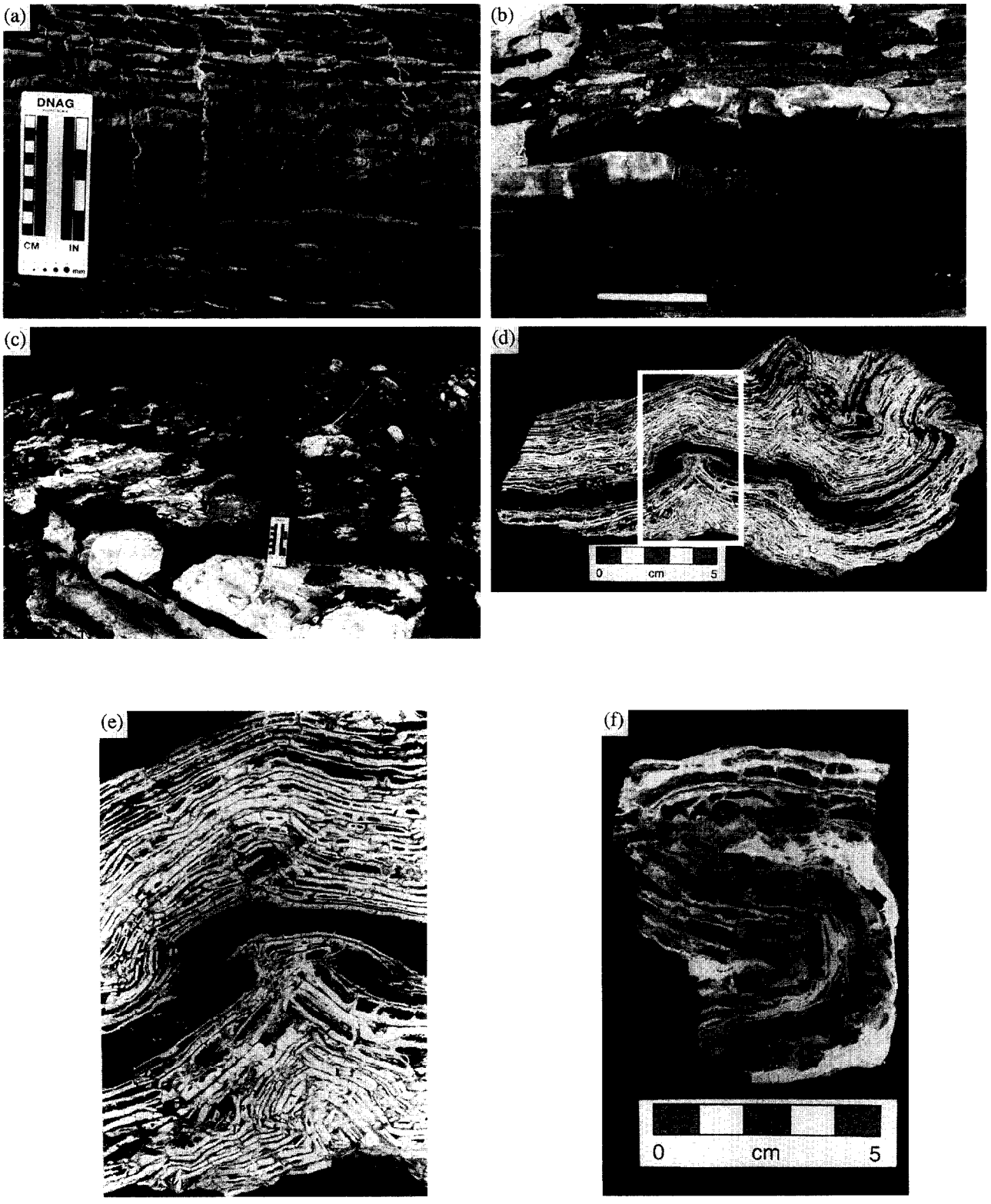

Fig. 7. Photographs of mesostructures in the Monterey Formation exposed in the southern Santa Maria basin. (a) Fracture partitioning in the organic phosphatic member at Lions Head, with opening-mode veining in the light limestone unit and normal faulting in underlying mudstone; normal faults belonging to this set were subsequently inverted; (b) carbonate bed in the mudstone unit of the organic phosphatic member at Lions Head showing inversion (b in Fig. 9); (c) Group I chert folds south of Purisima Point; note internal structure has been obliterated by subsequent transformation to black glassy opal-CT chert, although hinges are preserved as parallel ridges oriented ~03°/049°; (d) Group I chert fold with collapsed hinges; (e) close-up of the collapsed hinge zone; and (f) recumbent Group I chert folds, with axial planes parallel to bedding of enveloping surfaces (note boudinage).

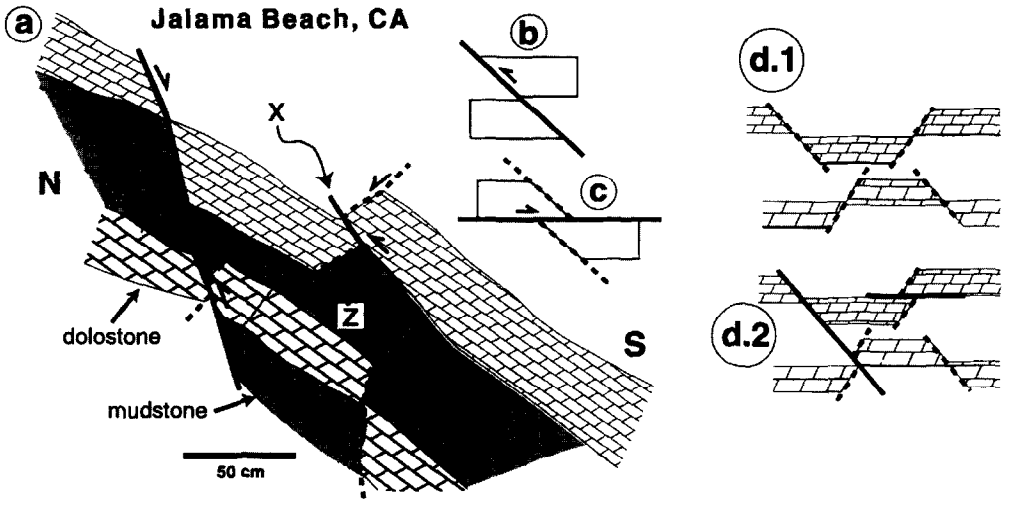

Fig. 8. (a) Outcrop sketch of inverted structure in the Monterey Formation at Jalama Beach, California. Dashed lines represent normal faults that have been subsequently inverted by reverse faults (thick solid lines). The high-angle fault to the north was originally a normal fault that underwent slight reverse reactivation (note displacement of pre-existing normal fault). The fault labeled 'x' offsets normal fault 'z'. The normal fault to the south may have been inverted, although no visible evidence is available to support inversion. Note the large amount of internal strain needed in mudstones to accommodate brittle deformation in the limestone beds. (b) Inversion geometry resulting from utilization of pre-existing normal fault plane. Note that in the absence of syn-sedimentation it is difficult to distinguish reverse faults from inverted normal faults. (c) Inversion resulting in normal fault transection and characterizing hangingwall and footwall cutoffs. (d) Two stages of sequential evolution of the described structure.

indicating a bimodal direction of transport. Figures 7(b) & 9(b) display the offset (referred to as 'decapitation' by Mitra, 1993) and rotation of a pre-existing normal fault in the hangingwall of the thrust. The listric shape and orientation of the fault-bounded footwall indicate this block was originally the hangingwall of a normal fault. In addition, whereas the carbonate bed in the upper portion of the sketch has been thrust-duplicated, the laminated mudstone in the lower portion remains offset in a normal sense, as discussed in Fig. 8. A single low-angle thrust and associated culmination fold is shown in Fig. 9(e). Planar, fault-bounded blocks rather than tapered edges at the culmination imply inversion of a normal fault structure (note offset of inferred dashed normal fault surface). A series of low-angle thrust duplexes appear in the upper portion of Fig. 9(f), along with a high-angle reverse fault that probably represents a reactivated normal fault. The complex geometry depicted in Fig. (9c) reveals numerous slip surfaces parallel to bedding. Our interpretation of the original configuration shows a limestone bed extended by a series of normal faults. A later phase of contraction then offset the original normal faults along bedding-parallel slip planes, duplicating and slightly rotating blocks of limestone. Figure 9(g) shows an east and west direction of transport for low-angle thrusts in limestone, similar to the lack of vergence observed in bedding-plane offsets in Fig. 9(c & d). Normal offsets in the lower portion of Fig. 9(g) indicate that the underlying mudstone unit did not invert, implying that shortening in mudstones must have been accommodated by other mechanisms such as distributed strain.

Orientation of Lions Head structures

Despite their wide range in orientation, normal faults in mudstones at Lions Head group into two apparently conjugate sets (Fig. 6b & c). Principal stress orientations were derived from the mean fault planes, assuming a conjugate origin and dip-slip motion consistent with localized dragged bedding adjacent to the faults, as well as other conjugate normal fault sets found in mudstone units along the Santa Barbara and Santa Maria coastlines (Gross, 1995; Gross and Engelder, 1995; Gross *et al.*, 1997). Effects of Pliocene–Recent folding were removed by rotating the vertically dipping beds back to horizontal around the regional fold axis (Fig. 6c, f, h & j). The WNW-extension orientation implied by the early syn- or pre-compactional normal faults is consistent with the generally E–W-trending extension that prevailed in the offshore Santa Maria basin during the Miocene (e.g. Crain *et al.*, 1985; McCulloch, 1989).

Cutoff geometries and orientations of displaced and folded carbonate beds were measured in order to determine the direction of shortening that prevailed during structural inversion (Fig. 6e–h). The field data consist of pairs of fault planes and cutoff bedding orientations for low-angle thrusts, pairs of bedding orientations for bed-parallel faults, slickenlines and sense of motion along fault planes when available, and the hinges of culmination and drag folds associated with low-angle thrusts and bedding-plane slip, respectively. The latter serve as excellent kinematic indicators of fault reactivation. The cutoff lines, which generally trend

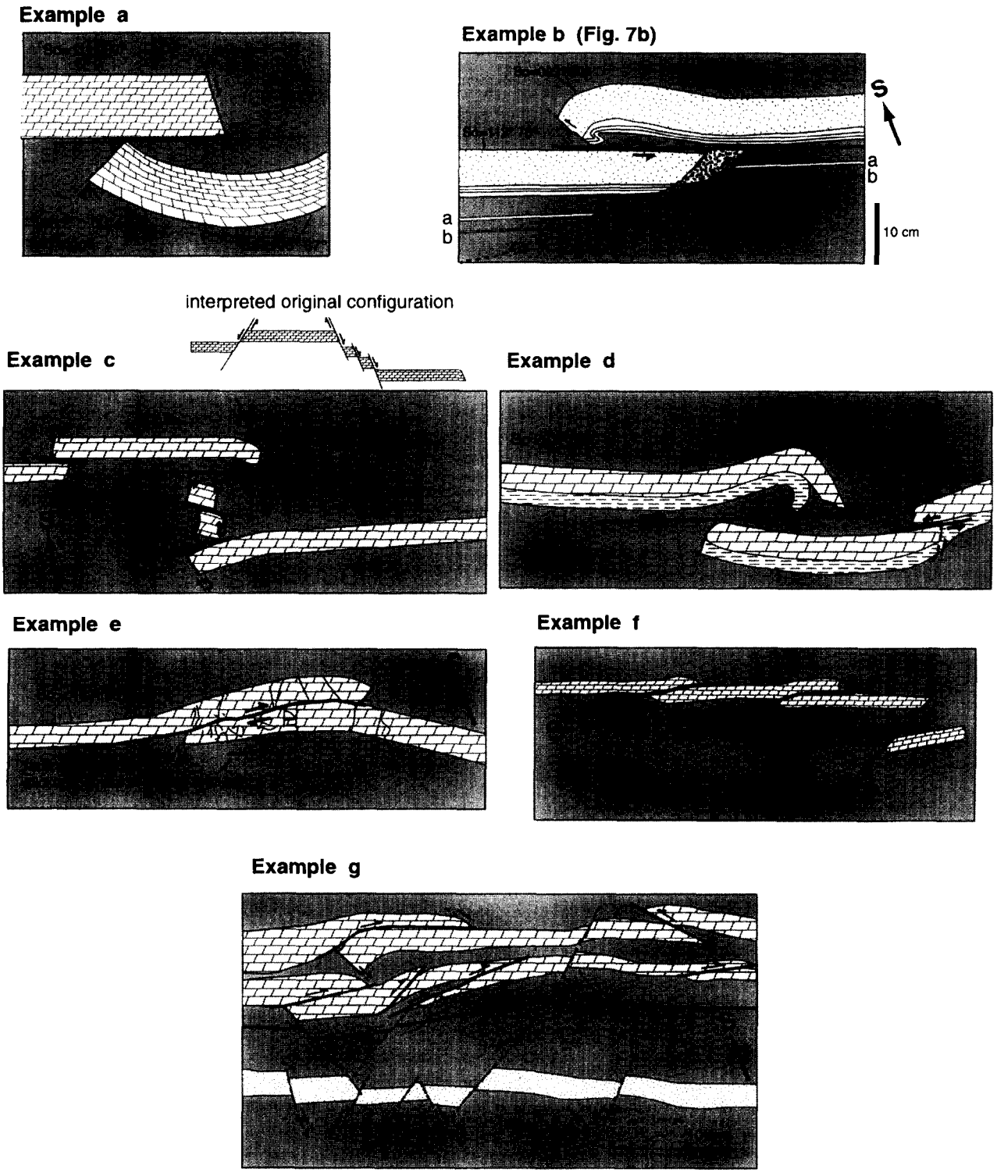

Fig. 9. Sketches of inverted structures at Lions Head. Key features to note are truncation of normal faults by low-angle thrusts (examples a, b, c, d, e and g), hangingwall drag folds (examples a, b and d), passive rotation of pre-existing normal faults (examples a, b and d), duplexes and culminations (examples e and g), and the role of bedding-plane slip in accommodating shortening (examples a, b, c, d and e). Refer to text for more details.

normal to direction of transport, scatter over a large area in the stereoplots (Fig. 6e & f), perhaps in part due to the wide range in orientation of the pre-existing normal faults. Upon restoring bedding to horizontal, the cutoffs span a 90° range in trend generally falling in the NE and SW quadrants of the stereoplots, thereby implying a general NW–SE shortening direction. Because the thrusts often utilized pre-existing normal fault planes during inversion, their cutoff lines do not provide very accurate kinematic information. A better constraint for shortening direction is provided by the more tightly clustered culmination and drag fold hinges (Fig. 6g & h). Upon removing the effect of late regional folding, the inversion-related culmination and drag folds are nearly horizontal with a mean trend of 18°/246°, further constraining the NW–SE contraction to an orientation of ~336°.

FOLDS

Folded beds of chert (i.e. chert folds) and fold-related structures in the Monterey Formation can be divided into three groups on the basis of orientation, geometry, interference patterns and correlation to other structures. Whereas inversion-related structures described above are restricted to the phosphatic member, chert folds are best observed up-section in the upper calcareous and clayey siliceous members (Fig. 2).

Group I folds

Group I folds and their related structures were observed at San Miguelito Canyon, Lompoc Landing, Purisima Point and Lions Head. These folds may display any number of characteristics including complete disaggregation of hinges and limbs, axial planes inclined parallel to enveloping surfaces (i.e. recumbent), hinges oblique to regional fold axes and evidence of refolding by a later contractional event.

Ridges of black glassy opal-CT chert south of Purisima Point (Fig. 7c) actually represent Group I fold hinges that formed prior to a diagenetic phase transformation. Here the original laminations were entirely obliterated due to replacement of opal-A with glassy opal-CT chert, yet outlines of box-shaped folds are clearly manifested as remnant bedding topography. Lack of continuity of individual beds is also a characteristic of Group I chert folds, as demonstrated by the disaggregation and collapse of hinge zones in Fig. 7(d & e). Note from the photographs that many chert layers were boudinaged prior to or during folding, similar to the pattern obtained experimentally by Kidan and Cosgrove (1996). In some instances the disaggregated chert folds are recumbent, with axial planes parallel or subparallel to bedding of enveloping surfaces (Fig. 7f). Several other unique structural features appear to have developed in conjunction with early folding. One such structural feature is formed by 5–20 cm long vertical axial-plane-parallel breccia zones that represent collapsed hinge zones of early folds. Hinges of Group I folds and related structures are refolded by a later phase of contraction, to form sinuous ridge-like structures in outcrop (Fig. 10). Another group of related features are chert wedges that protrude from pure siliceous horizons into neighboring porcellanites. Behl and Garrison (1994) provide three possible mechanisms of formation for these 'dike' structures, all of which reflect an interconnection between diagenesis and deformation. Both Grivetti (1982) and

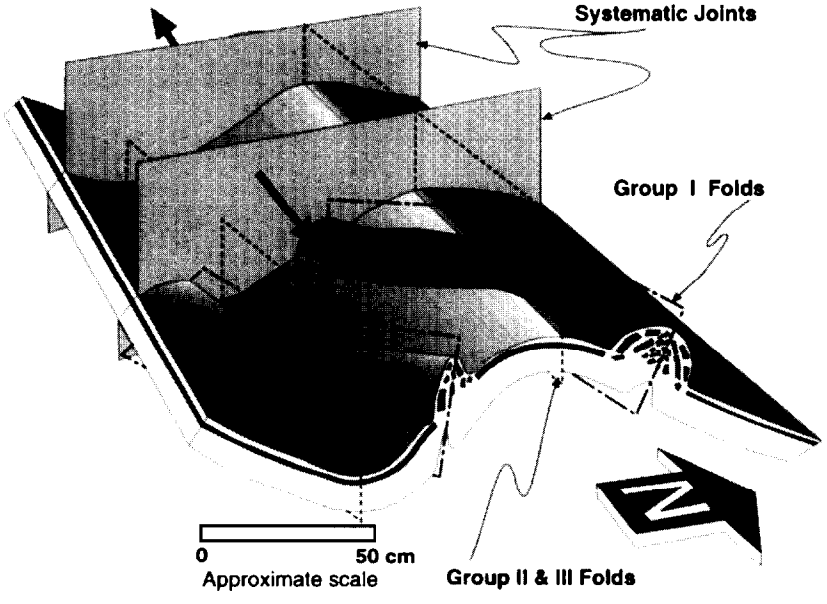

Fig. 10. Sketch demonstrating relationships between early folds, late folds and systematic joints. Brecciated early fold hinges form sinuous ridges that are refolded by a later contractional deformation episode. Late regional folding resulted in the development of hinge-normal systematic joints.

Behl and Garrison (1994) recognized that lineations on bedding surfaces created by these chert wedges were later rotated passively upon folding.

All Group I fold and fold-related structures display similar orientations at a given locality. Combined data from Purisima Point and Lompoc Landing, where bedding ranges from horizontal to moderately dipping, yield a horizontal NE–SW mean Group I fold axis (Fig. 5c). While both Group I and regional fold axes are horizontal, they are oblique to one another, with Group I fold hinges oriented ~48° counterclockwise from the regional fold axis (Fig. 10). Furthermore, Group I fold hinges are oblique to the dominant systematic joint set (Figs 5 & 10). Similar angular relationships were observed throughout the basin. At San Miguelito Canyon we measured axial planes of recumbent Group I folds in addition to their hinges (Fig. 4). Group I fold hinges at San Miguelito Canyon (Fig. 4), Purisima Point, Lompoc Landing (Fig. 5) and Lions Head (Fig. 6h & i) display consistent NE–SW-trending horizontal hinges after restoration of bedding to horizontal, indicating their formation prior to subsequent regional folding. In addition, Group I fold hinges observed in the upper calcareous–siliceous member at Lions Head are roughly aligned with cutoff lines and culmination/drag folds associated with inversion structures in the phosphatic member (Fig. 6).

Group II folds

The most prominent mesoscopic structures in the Monterey Formation are the Group II chert folds, which often appear as detached fold trains confined to silica-rich mechanical units. These disharmonic chert folds are detached from adjacent units by thin clay layers or simply due to sharp contrasts in mechanical properties between pure siliceous cherts and detritus-rich mudstones and porcellanites. In contrast to Group I folds, Group II chert folds are not accompanied by related axial-planar breccia zones and chert wedges. Group II folds typically involve more layers (i.e. thicker folded sections) and display much greater amplitudes than Group I folds. They are highly cylindrical with interlimb angles ranging from gentle to isoclinal, and shapes varying from symmetric box-folds to asymmetric overturned folds. Whereas Group I folds may exhibit subhorizontal axial planes and complete disaggregation of limbs and hinges, axial planes of Group II folds are mostly subperpendicular to their enveloping surfaces (i.e. bedding in adjacent porcellanites and mudstones). Non-symmetric Group II folds do not display a consistent sense of vergence, a feature also noted by Grivetti (1982). In addition, Group II folds at most display only partial disaggregation of bedding, often in the hinge zone in response to the development of fault-propagation folds. However, despite occasional hinge collapse, fold limbs remain entirely intact.

An example of a Group II chert fold at Lions Head is shown in Fig. 11(a). The glassy chert unit is detached from the underlying steeply dipping mudstone. Note the symmetrical shape, extreme tightness of folding (isoclinal to obtuse) and axial plane normal to mudstone bedding. A typical box-fold geometry displaying orthogonal limbs appears in Fig. 11(b). In both examples individual layers remain intact after folding, perhaps due to subsequent diagenetic overprinting. One important characteristic typical of contorted chert beds at Lions Head, Purisima Point and Lompoc Landing is that fold amplitude, which results in an ~2–5 times increase in

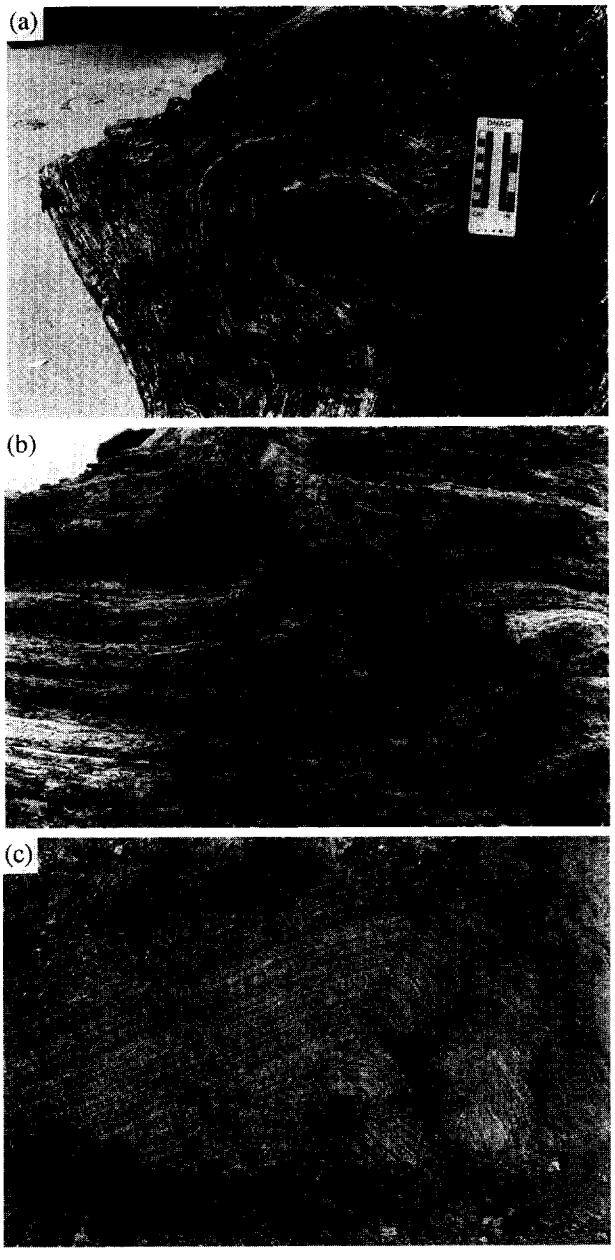

Fig. 11. Photographs of late folds (Groups II and III) in the Monterey Formation. (a) Detached Group II chert fold in the upper calcareous siliceous member at Lions Head. Note symmetry, axial plane normal to bedding of underlying shale, and extreme tightness of the hinge zone. (b) Symmetric Group II box-folds in the upper calcareous siliceous member at Lompoc Landing. (c) Outcrop-scale fault-propagation fold (Group III) with S-vergence at Sweeney Road (enlarged box in Fig. 3).

bed thickness, remains consistent in height irrespective of structural position. In other words, orthogonal thicknesses of contorted chert beds on limbs of regional folds are approximately the same as thicknesses in hinge zones.

Despite their wide variety of shapes, geometries and vergence, Group II chert folds trend consistently ESE–WNW throughout the southern onshore Santa Maria basin, which in turn corresponds to regional fold axes derived from π-diagrams (Figs 5 & 6). At Lions Head, the Group II chert folds plunge in accord with the WSW-plunging regional fold axis (Fig. 6k). Subhorizontal chert fold hinges plunge in a shallow manner to the east-southeast at Purisima Point and Lompoc Landing, where regional fold axes are also slightly ESE plunging (Fig. 5a & c). Thus, disharmonic Group II chert folds are aligned with the regional fold trend. As shown schematically in Fig. 10, Group I structures are obliquely refolded by Group II chert folds. Furthermore, Group II chert fold hinges are aligned precisely with poles to the dominant NNE–SSW joint set (Fig. 5b).

Group III folds and thrust faults

In contrast to the symmetrical nature and lack of consistent vergence for Group II folds, Group III folds observed in the clayey siliceous member at Sweeney Road and San Miguelito Canyon display a dominant S-directed vergence, characterized by steep to overturned short southern limbs and shallower upright limbs on northern flanks. Outcrop sketches of Sweeney Road and San Miguelito Canyon demonstrate the dependence of folding on faulting (Fig. 3). Note the consistent S-vergence of thrusting in these sections, as well as our interpretation of subsurface blind thrusts to account for several meter-scale folds. Many of the faults themselves have been folded attesting to on-going contraction.

Group III chert folds generally develop as a result of either bedding-plane detachments (disharmonic fold trains) or thrusts splaying off detachments (fault-bend and fault-propagation folds). An example of the latter, depicted schematically in Box A of Fig. 3, can be seen in the photograph in Fig. 11(c). Chert fold hinges plunge gently to the ESE at San Miguelito Canyon (Fig. 4) and Sweeney Road (Fig. 3), and hence are parasitic to regional fold axes, which are similarly gently ESE plunging. In addition, cutoff lines at Sweeney Road, representing intersections of fault planes with bedding or two bedding planes juxtaposed across a detachment, are aligned precisely with the small chert fold hinges and the regional fold axis.

DISCUSSION

The style, distribution and geometry of mesoscopic structures in the Monterey Formation result from the interaction of several key factors such as rheology, diagenesis and applied tectonic forces. Despite its relatively young age, the Monterey Formation exhibits a large and varying collection of deformation features, including ptygmatically folded veins, normal faults, detachment and thrust faults, boudinaged chert layers, inverted normal faults and folds belonging to three separate groups. Having established the geometries and orientations of these structures, we now attempt to reconstruct a Miocene–Holocene deformation history for the southern Santa Maria basin.

Effects of silica diagenesis on structural interpretation

We must emphasize that effects of silica diagenesis add complexity to the structural interpretation of folds in the Monterey Formation and similar siliceous rocks, as acknowledged by previous workers (e.g. Kolodny, 1967; Redwine, 1981; Steinitz, 1981; Grivetti, 1982; Fink and Reches, 1983; Snyder *et al.*, 1983; Dunham and Blake, 1987; Snyder, 1987; Behl and Garrison, 1994). The process of silica diagenesis begins from deposition and lasts either until sediments reach maximum burial or silica is converted to the stable quartz phase (e.g. Jones and Segnit, 1971; Murata and Larson, 1975; Isaacs, 1980; Behl and Garrison, 1994). Thus, diagenesis spans millions of years and occurs synchronously with tectonic deformation, and consequently earlier-formed structures are often overprinted by a later phase of diagenesis (see Figs 7c & 12) (e.g. Snyder *et al.*, 1983; Dunham and Blake, 1987; Stock, 1992). In addition, dramatic changes in physical properties such as porosity, density and elastic moduli accompany silica phase transformations (e.g. Isaacs, 1981; Gross *et al.*, 1995). Most importantly, the addition of large amounts of silica, and hence dilation of chert beds, may have provided a mechanism for fold development that does not necessarily require tectonic contraction.

Fold geometry, bed length, orthogonal thickness and cleavage may help distinguish between diagenetic-related folding and folding caused by tectonic shortening at

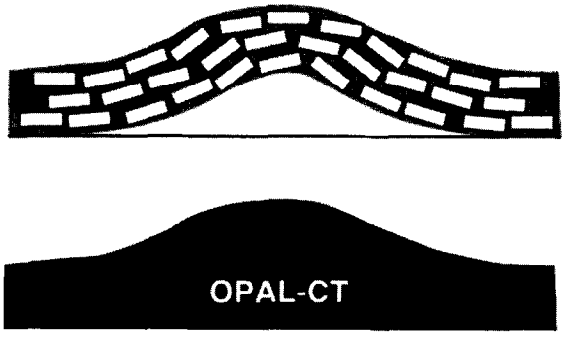

Fig. 12. Sketch demonstrating how diagenetic phase transformations can mask pre-existing structures. (a) Early deformation resulted in the boudinage and rotation of blocks during folding. (b) Transformation to black opal-CT chert overprinted original internal structures, although remnant fold hinges remain intact as linear ridges. See photograph in Fig. 7(c).

Lions Head. When large quantities of silica are added to laterally constrained chert beds, they buckle into fold trains in order to accommodate their increase in volume (Fig. 13a). When bed lengths are straightened out, the contorted chert beds are considerably longer than adjacent, lower-amplitude non-chert horizons, indicating an increase in bed length during folding. A second key observation is that beds of contorted chert maintain a uniform and increased thickness independent of structural position (Fig. 13a); if the folds were purely of tectonic origin, then thickening in hinge zones should be compensated by thinning in limbs in order to maintain bed length (Fig. 13c). Third, during volume expansion folding there is no systematic direction of transport between limbs as is the case for flexural-slip or flexural-flow folding. Thus, diagenetic folds are symmetrical and upright, with axial planes normal to enveloping surfaces or slightly inclined without any consistent vergence. In folds of tectonic origin, however, parasitic folds will display a sense of vergence and hence inclined axial planes occur on limbs in addition to a similar fold geometry to accommodate hinge zone thickening (Fig. 13c) (A. Becker, personal communication). Furthermore, intense tectonic shortening should result in layer-parallel shortening with cleavage development in adjacent non-folded detritus-rich beds. As described earlier, contorted chert beds at Lions Head to a large extent resemble Fig. 13(a) and, in the absence of pronounced axial-planar cleavage in adjacent beds, we conclude that a large component of folding at Lions Head is attributable to diagenetic processes. Upon close inspection of contorted beds, one observes that each chert layer is composed of boudins with silica cemented in between gaps, thereby adding to the effective bed length. The boudins exhibit extension normal to fold hinges (Fig. 13b), further evidence in favor of localized net dilation.

Although diagenesis plays a major role in the development of some chert folds, we believe that folds and inverted faults at Lions Head indeed record an episode of tectonic contraction, and hence inversion, for the following reasons. First, there is a strong similarity in hinge orientation between Group II folds at Lions Head, Purisima Point and Lompoc Landing and Group III folds at Sweency Road and San Miguclito Canyon. Considering that Group III folds clearly represent tectonic deformation (see below) and are found in opal-CT rocks (i.e. they did not experience large silica influxes due to quartz transformation), then it is likely that similarly oriented Group II folds are recording the same tectonic signal. Second, Behl (1992) measured 20% internal finite shortening within non-folded diatomites of the Monterey Formation near Lompoc, California; and, third, numerous thrusts and inverted normal faults have been observed on seismic lines in the onshore and

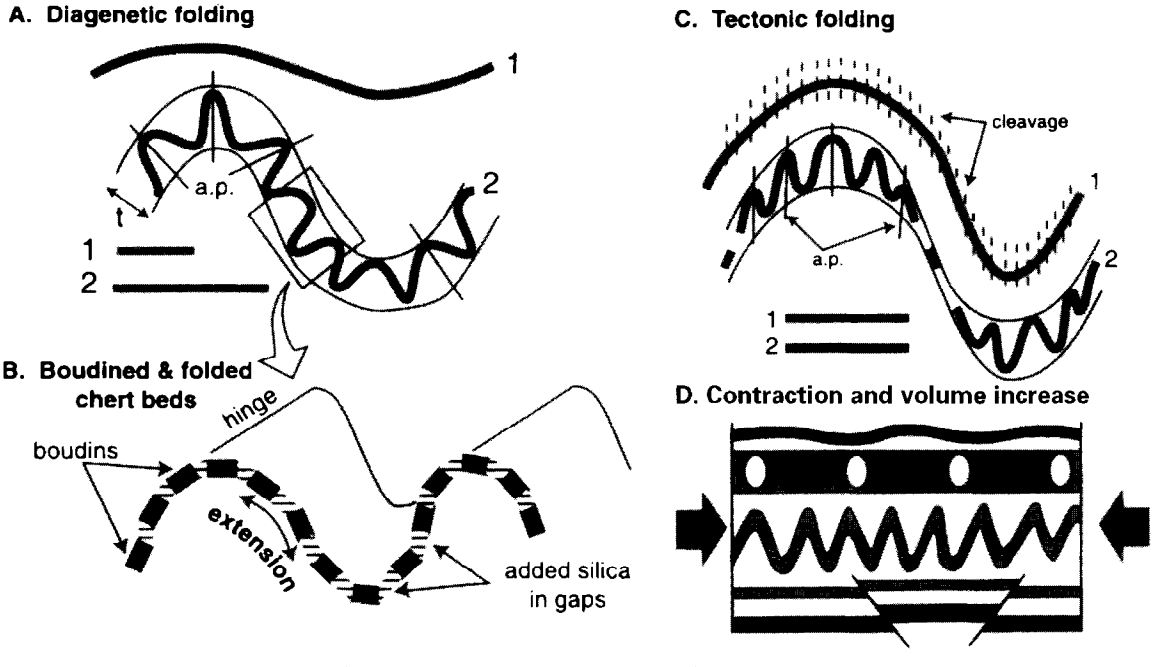

Fig. 13. Sketch depicting contributions of diagenesis and tectonic shortening to the development of contorted chert beds in the Monterey Formation. (a) Folding due primarily to diagenetic effects. Note symmetric folds, lack of vergence, axial planes (a.p.) normal to enveloping surface and uniform thickness of contorted unit regardless of structural position. Restored chert bed (2) is significantly longer than restored mudstone (1) due to addition of silica. (b) Close-up of chert bed in (a) demonstrating how the precipitation of diagenetic silica in boudin gaps results in the lengthening of the bed. (c) Expected structural geometries for folding due entirely to tectonic shortening. Parasitic chert folds show consistent sense of vergence, asymmetry and axial planes oblique to enveloping surfaces. Thickening in hinge zones is balanced by thinning in limbs in order to maintain original bed length. Intense folding may lead to cleavage development in detritus-rich beds. In the absence of cleavage, final bed lengths should equal original bed lengths. (d) Our mechanism for mesostructure development in the Monterey Formation includes a combination of tectonic shortening and diagenetic effects.

offshore Santa Maria basins (e.g. Crouch *et al.*, 1984; Namson and Davis, 1990; Clark *et al.*, 1991; McIntosh *et al.*, 1991).

Established relations among structures

Detailed field observations reveal three sets of folds which differ from each other on the basis of orientation, geometry, and relations to regional folding, regional jointing and thrusting. The temporal development of Group I folds is constrained by axes oblique to actively developing regional fold axes and poles to systematic joints, and hinges refolded by both Group II and Group III folds. Group II folding occurred in conjunction with silica diagenesis, whereas Group III folds are unaffected by diagenesis. Evidence for a syn-diagenetic origin for Group II folds include significant volume increase during folding, intense folding restricted to beds of high-silica purity at more advanced stages of diagenesis, and overprinting and healing of fracture-related folds by subsequent diagenesis. Group III folds are associated with regional folding as manifested by: (1) geometries consistent with regional thin-skinned detachment folding (Namson and Davis, 1990); (2) axes parallel to thrust cutoff lines; (3) axes parallel and, hence, parasitic to $\sim 095^{\circ}$ regional fold axes; (4) vergence consistent with S-directed transport; and (5) axes normal to the dominant systematic joint set. The dominant joint set found in the Monterey Formation is normal to bedding and strikes NNE–SSW (e.g. Belfield *et al.*, 1983; Gross, 1983; Narr and Suppe, 1991). These joints accommodate strike-parallel extension in response to tectonic contraction, and consequently are oriented normal to regional fold axes (Fig. 10) (e.g. Gross and Engelder, 1995). Owing to their similar orientations and relations to regional fold axes, we believe that Group II and Group III folds formed within the same tectonic stress fields; differences between the two groups are due to deeper burial, and hence more advanced diagenesis at Lions Head, Purisima Point and Lompoc Landing.

Sequence of deformation recorded in the Monterey Formation

In light of structural data and relations established above, we present a chronology of deformation in the southern Santa Maria basin for the past 15 Ma. Deposition of the Monterey Formation began during the early–middle Miocene in a deep basin along the margin of the California borderland. Nutrient-rich upwelling waters, anoxic conditions at depth and high rates of deposition led to the accumulation of finely laminated sediments rich in biogenic opal-A (Fig. 14a). Prior to full compaction the Monterey Formation experienced a phase of tectonic extension in the mid–late Miocene, consistent with the regional tectonic stress regime (Crain *et al.*, 1985; McCulloch, 1989; Nicholson *et al.*, 1992). The style of extensional deformation varied according to lithology, with normal faults developing in mudstones, opening-mode veins in carbonates and boudinage in thinly laminated siliceous units (Fig. 14b). The package of sediments was then subjected to vertical compaction during burial, apparently in the absence of high horizontal compressive stresses. During compaction veins were ptygmatically folded (Fig. 7a), normal faults rotated passively and chocolate tablet boudinage developed in thinly laminated siliceous beds (Gross, 1995) (Fig. 14c). An initial phase of tectonic contraction ensued in the early Pliocene as a result of the switch from regional transtension to regional transpression (e.g. Hornafius, 1985; Harbert and Cox, 1989). This contraction resulted in the inversion of normal faults in mudstone units and syn-diagenetic folding in siliceous layers as basin subsidence continued (Fig. 14d). As a consequence, the transport direction of structures related to inversion such as fault cutoff lines, culmination folds and drag folds correspond to Group I fold axes. Early contraction was accomplished through regional layer-parallel shortening rather than regional folding; when bedding at Lions Head is restored to horizontal, inverted structures in the phosphatic member, as well as Group I folds, assume a horizontal attitude indicating the early contractional event predated regional folding. The final phase of deformation, which continues today, is an intensification of tectonic contraction that began at ~ 2–4 Ma with the development of the Santa Maria fold-and-thrust belt (Namson and Davis, 1990). Regional fault-related detachment folding resulted in ESE–WNW-trending regional fold axes, parasitic Group II and III chert folds in the Monterey Formation, and the refolding of earlier Group I structures (Fig. 14e). A systematic fracture system developed in conjunction with the fold-and-thrust belt, with the dominant joint set oriented normal to regional fold axes.

Significance of inverted faults and relation to km-scale structures

The strongest geological evidence in favor of structural inversion is sedimentary thickening across faults that were reactivated in reverse (e.g. Cooper and Williams, 1989; Buchanan and Buchanan, 1995). However, inversion can occur in the absence of growth faulting, further complicating structural interpretations. We believe that mesoscale inverted structures in the Monterey Formation may provide insight into understanding basin-scale inversion, especially in strata with high contrasts in mechanical properties. Key features to observe on geological maps and seismic sections include truncated and rotated normal faults, thrust duplication and drag/culmination folds associated with contraction along detachments, and unique geometries (especially dip directions) of hangingwall and footwall cutoffs.

Indeed, small inverted structures observed in the

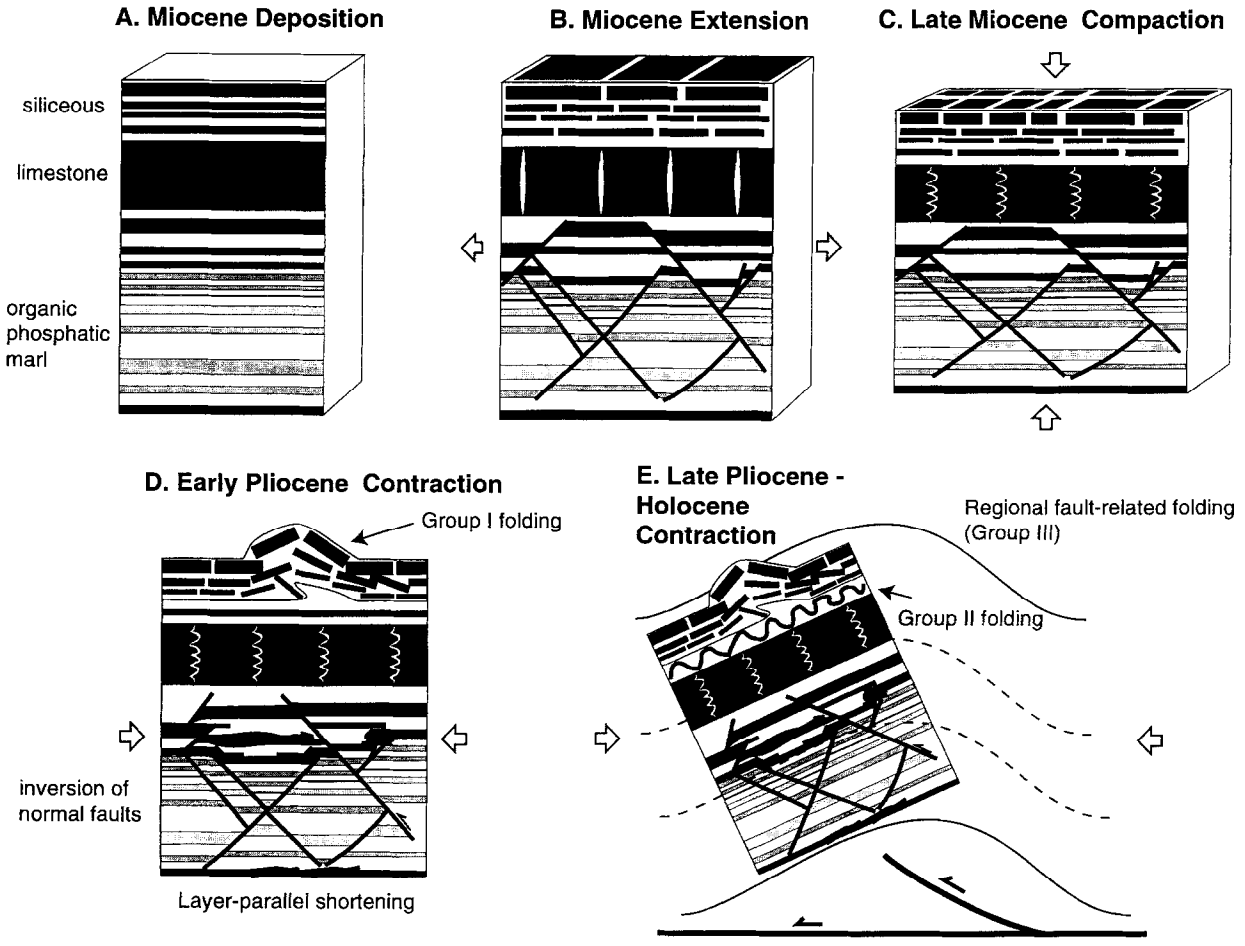

Fig. 14. Model depicting sequence and timing of deformation events and mesostructures that developed in the Monterey Formation from middle Miocene to the present.

Monterey Formation are mirrored by numerous km-scale, basin-bounding Miocene growth faults that were subsequently inverted during Pliocene–Holocene contraction, including the offshore Queenie structure (Clark *et al.*, 1991; McIntosh *et al.*, 1991), the Hosgri fault (e.g. Crouch *et al.*, 1984; Namson and Davis, 1990) and the onshore Orcutt fault (Namson and Davis, 1990). Small inverted structures provide geometric details and constraints on the timing of deformation that are unattainable from seismic lines or regional cross-sections. For example, mesoscopic structures within the Monterey Formation attest to two temporally and structurally different phases of tectonic contraction within the southern Santa Maria basin. Furthermore, S-directed folds and thrusts observed at Sweeney Road and San Miguelito Canyon coincide in vergence with the Namson and Davis (1990) regional detachment at ~8–10 km depth. The lack of a consistent vergence for chert folds at Lions Head, Purisima Point and Lompoc Landing may result from the Purisima–Solomon backthrust, which superimposes local N-directed transport on regional S-vergence (Namson and Davis, 1990), as well as the large component of bed lengthening due to syn-diagenetic folding.

CONCLUSIONS

The style of deformation in the Monterey Formation depends to a large extent upon lithology, as different structures (e.g. faults vs veins, inverted faults vs folds) developed in response to the same applied tectonic forces. Structural inversion of normal faults within mudstone units of the Monterey Formation resulted in the development of several characteristic geometries, including normal faults truncated and rotated by bedding-plane detachments, low-angle thrusts, thrust duplexes, drag folds, culmination folds and normal faults reactivated in reverse. Removing effects of diagenesis and combining data from these structures with geometries and orientations of three groups of folds found at other stratigraphic levels in the Monterey Formation, a chronology of Neogene deformation within the southern Santa Maria basin emerges. Miocene extension is followed by two phases of contraction that invert the basin. Early

Pliocene layer-parallel contraction resulted in the inversion of normal faults within mudstone mechanical units and the development of Group I chert folds in siliceous beds. Late Pliocene–Holocene contraction resulted in the development of the Santa Maria fold-and-thrust belt and a later phase of parasitic chert folds (Groups II and III) within the Monterey Formation. The two phases of contraction recorded in the Monterey Formation support the notion that layer-parallel shortening precedes the development of fold-and-thrust belts in compressional tectonic regimes, as is the case for the Appalachian Plateau and Valley and Ridge provinces (Engelder and Engelder, 1977; Engelder and Geiser, 1980).

Acknowledgements—We thank Wendy Bartlett, Richard Behl, Mark Fischer, Gren Draper and Taixu Bai for critical input and very helpful discussions, and we salute Alexander Becker for insights into fold development. Reviews by L. Tennyson, T. Flöttmann and R. J. Norris improved the paper and are gratefully appreciated. Acknowledgement is made to the Donors of The Petroleum Research Fund, administered by the American Chemical Society, for the support of this research through PRF Grant 28338-GB2; DGICYT grant PB-93-1149 C03-02 and additional funding was provided by a research grant from the University of Salamanca.

REFERENCES

Argand, E. (1911) *Les Nappes de Recouvrement des Alpes Pennines et Leurs Prolongements Structuraux*. Materiali per la Carta Geologica della Svizzera.

Bally, A. W. (1984) Tectonogenese et sismique reflection. *Bulletin de la Société géologique de la France* **26**, 279–286.

Behl, R. J. (1992) Chertification in the Monterey Formation of California and deep-sea sediments of the West Pacific. Unpublished Ph.D. thesis, University of California, Santa Cruz.

Behl, R. J. and Garrison, R. E. (1994) The origin of chert in the Monterey Formation of California (USA). In *Proceedings of the 29th International Geological Congress*, eds A. Iijima *et al.*, Part C, pp. 101–132. V.S.P., The Netherlands.

Belfield, W. C., Helwig, J., LaPointe, P. and Dahleen, W. K. (1983) South Ellwood oil field, Santa Barbara Channel, California, a Monterey Formation Fractured Reservoir. In *Petroleum Generation and Occurrence in the Miocene Monterey Formation, California*, eds C. M. Isaacs and R. E. Garrison, pp. 213–222. Pacific Section of the Society of Economic Paleontogists and Mineralogists Special Publication **17**.

Bramlette, M. N. (1946) *The Monterey Formation of California and the Origin of its Siliceous Rocks*. U.S. Geological Survey Professional Paper **212**.

Buchanan, J. G. and Buchanan, P. G. (eds) (1995) *Basin Inversion*. Geological Society of London Special Publication **88**.

Butler, R. W. H. (1989) The influence of pre-existing basin structure on thrust system evolution in the Western Alps. In *Inversion Tectonics*, eds M. A. Cooper and G. D. Williams, pp. 105–122. Geological Society of London Special Publication **44**.

Cartwright, J. A. (1989) The kinematics of inversion in the Danish Central Graben. In *Inversion Tectonics*, eds M. A. Cooper and G. D. Williams, pp. 153–176. Geological Society of London Special Publication **44**.

Chapman, T. J. (1989) The Permian to Cretaceous structural evolution of the Western Approaches Basin (Melville sub-basin), UK. In *Inversion Tectonics*, eds M. A. Cooper and G. D. Williams, pp. 177–200. Geological Society of London Special Publication **44**.

Clark, D. H., Hall, N. T., Hamilton, D. H. and Heck, R. G. (1991) Structural analysis of late Neogene deformation in the central offshore Santa Maria Basin. *Journal of Geophysical Research* **96**, 6435–6458.

Compton, J. S. (1991) Porosity reduction and burial history of siliceous rocks from the Monterey and Sisquoc Formations, Point Pedernales area, California. *Bulletin of the Geological Society of America* **103**, 625 636.

Cooper, M. A. and Williams, G. D. (eds) (1989) *Inversion Tectonics*. Geological Society of London Special Publication **44**.

Cox, A. and Engebretson, D. (1985) Change in motion of the Pacific plate at 5 Myr B.P *Nature* **313**, 472–474.

Crain, W. E., Mero, W. E. and Patterson, D. (1985) Geology of the Point Arguello discovery. *Bulletin of the American Association of Petroleum Geologists* **69**, 537–545.

Crouch, J. K. (1979) Neogene tectonic evolution of the California Continental borderland and western Transverse Ranges. *Bulletin of the Geological Society of America* **90**, 338–345.

Crouch, J., Bachman, S. B. and Shay, J. T. (1984) Post-Miocene compressional tectonics along the central California margin. In *Tectonics and Sedimentation Along the California Margin*, eds J. Crouch and S. B. Bachman, pp. 37–54. Pacific Section of the Society of Economic Paleontogists and Mineralogists **38**.

Crouch, J. K. and Suppe, J. (1993) Late Cenozoic tectonic evolution of the Los Angeles basin and inner California borderland: A model for core complex-like crustal extension. *Bulletin of the Geological Society of America* **105**, 1415–1434.

Cummings, D. and Johnson, T. A. (1994) Shallow geologic structure, offshore Point Arguello to Santa Maria River, central California. In *Seismotectonics of Central California Coast Ranges*, ed. I. B. Alterman, R. B. McMullen, L. S. Cluff and D. B. Slemmons, pp. 211–222. Geologial Society of America Special Paper **292**.

Dibblee, T. W., Jr (1988a) *Geologic Map of the Lompoc Hills and Point Conception Quadrangles*. Dibblee Geological Foundation Map No. DF-18.

Dibblee, T. W., Jr (1988b) *Geologic Map of the Tranquillon Mtn. and Point Arguello Quadrangles*. Dibblee Geological Foundation Map No. DF-19.

Dibblee, T. W., Jr (1988c) *Geologic Map of the Lompoc and Surf Quadrangles*. Dibblee Geological Foundation Map No. DF-20.

Dibblee, T. W., Jr (1989a) *Geologic Map of the Casmalia and Orcutt Quadrangles*. Dibblee Geological Foundation Map No. DF-24.

Dibblee, T. W., Jr (1989b) *Geologic Map of the Point Sal and Guadalupe Quadrangles*. Dibblee Geological Foundation Map No. DF-25.

Dunham, J. B. and Blake, G. H. (1987) Guide to coastal outcrops of the Monterey Formation of western Santa Barbara County, California. In *Guide to Coastal Outcrops of the Monterey Formation of Western Santa Barbara County, California. Field Trip Guide*, ed. J. B. Dunham, pp. 1–36. Pacific Section of the Society of Economic Paleontogists and Mineralogists **35**.

Engelder, T. and Engelder, R. (1977) Fossil distortion and decollement tectonics of the Appalachian Plateau. *Geology* **5**, 457–460.

Engelder, T. and Geiser, P. A. (1980) On the use of regional joint sets as trajectories of paleostress fields during the development of the Appalachian Plateau, New York. *Journal of Geophysical Research* **85**, 6319–6341.

Fink, J. H. and Reches, Z. (1983) Diagenetic density inversions and the deformation of shallow marine chert beds in Israel. *Sedimentology* **30**, 261–271.

Glennie, K. W. and Boegner, P. L. E. (1981) Sole pit inversion tectonics. In *Petroleoum Geology of the Continental Shelf of Europe*, eds L. V. London and G. D. Hobson, pp. 110–120. Institute of Petroleum.

Grier, M. E., Salfity, J. A. and Allmendinger, R. W. (1992) Andean reactivation of the Cretaceous Salta rift, northwestern Argentina. *Journal of South American Earth Sciences* **5**, 351–372.

Grivetti, M. C. (1982) Aspects of stratigraphy, diagenesis, and deformation in the Monterey Formation near Santa Maria–Lompoc, California. MA thesis, University of California, Santa Barbara.

Gross, M. R. (1983) The origin and spacing of cross joints: examples from the Monterey Formation, Santa Barbara coastline, California. *Journal of Structural Geology* **15**, 737–751.

Gross, M. R. (1995) Fracture partitioning: failure mode as a function of lithology in the Monterey Formation of coastal California. *Bulletin of the Geological Society of America* **107**, 779–792.

Gross, M. R. and Engelder, T. (1995) Strain accommodated by brittle failure in adjacent units of the Monterey Formation, U.S.A.: scale effects and evidence for uniform displacement boundary conditions. *Journal of Structural Geology* **17**, 1303–1318.

Gross, M. R., Fischer, M. P., Engelder, T. and Greenfield, R. J. (1995) Factors controlling joint spacing in interbedded sedimentary rock: integrating numerical models with field observations from the

Monterey Formation, USA. In *Fractography: Fracture Topography as a Tool in Fracture Mechanics and Stress Analysis*, ed. M. S. Amen, pp. 215–233. Geological Society of London Special Publication **92**.

Gross, M. R., Gutiérrez-Alonso, G., Bai, T., Wacker, M. A., Collinsworth, K. B. and Behl, R. J. (1997) Influence of mechanical stratigraphy and kinematics on fault scaling relations. *Journal of Structural Geology* **19**, 171–183.

Hall, C. A. (1981) San Luis Obispo Transform Fault and Middle Miocene rotation of the western Transverse Ranges, California. *Journal of Geophysical Research* **86**, 1015–1031.

Harbert, W. and Cox, A. (1989) Late Neogene motion of the Pacific plate. *Journal of Geophysical Research* **94**, 3052–3064.

Hayward, A. B. and Graham, R. H. (1989) Some geometrical characteristics of inversion. In *Inversion Tectonics*, eds M. A. Cooper and G. D. Williams, pp. 17–40. Geological Society of London Special Publication **44**.

Hornafius, J. S. (1985) Neogene tectonic rotation of the Santa Ynez Range, Western Transverse Ranges, California, suggested by paleomagnetic investigation of the Monterey Formation. *Journal of Geophysical Research* **90**(B14), 12503–12522.

Howell, D. G., Crouch, J. K., Greene, H. G., McCulloch, D. S. and Vedder, J. G. (1980) Basin development along the late Mesozoic and Cenozoic California margin; A plate tectonic margin of subduction, oblique subduction, and transform tectonics. In *Sedimentation in Oblique-slip Mobile Zones*, eds P. F. Ballance and H. G. Reading, pp. 43–62. International Association of Sedimentologists Special Publication **4**.

Isaacs, C. M. (1980) Diagenesis in the Monterey Formation examined laterally along the coast near Santa Barbara, California. Unpublished Ph.D. thesis, Stanford University.

Isaacs, C. M. (1981) Outline of diagenesis in the Monterey Formation examined laterally along the Santa Barbara coast, California. In *Guide to the Monterey Formation in the California Coastal Area, Ventura to San Luis Obispo*, ed. C. M. Isaacs, pp. 25–38. Pacific Section of the American Association of Petroleum Geologists **52**.

Isaacs, C. M. (1982) Influence of rock composition on kinetics of silica phase changes in the Monterey Formation, Santa Barbara area, California. *Geology* **10**, 304–308.

Isaacs, C. M. (1983) Compositional variation and sequence in the Miocene Monterey Formation, Santa Barbara coastal area, California. In *Cenozoic Marine Sedimentation, Pacific Margin, U.S.A.*, eds D. K. Lame and R. J. Steel, pp. 117–132. Pacific Section Society of Economic Paleontologists and Mineralogists Special Publication.

Jackson, J. A. (1980) Reactivation of basement faults and crustal shortening in orogenic belts. *Nature* **283**, 343–346.

Jennings, C. W. (1977) *Geologic Map of California*. State of California Division of Mines and Geology, Geologic Data Map No. 2.

Jones, J. B. and Segnit, E. R. (1971) The nature of opal: I. Nomenclature and constituent phases. *Journal of the Geological Society of Australia* **18**, 56–68.

Kidan, T. W. and Cosgrove, J. W. (1996) The deformation of multilayers by layer-normal compression; an experimental investigation. *Journal of Structural Geology* **18**, 461–474.

Kolodny, Y. (1967) Lithostratigraphy of the Mishash Formation, Northern Negev. *Israel Journal of Earth Sciences* **16**, 57–73.

Luyendyk, B. P., Kamerling, M. J. and Terres, R. (1980) Geometric model for Neogene crustal rotations in southern California. *Bulletin of the Geological Society of America* **91**, 211–217.

MacKinnon, T. (1989) *Oil in the California Monterey Formation; 28th International Geological Congress Field Trip Guidebook T311*. American Geophysical Union, Washington, DC.

Martínez-Catalán, J. R., Hacar Rodriguez, M. P., Villar Alonso, P., Pérez-Esta, A. and González Lodeiro, F. (1992) Lower Paleozoic extensional tectonics in the limit between the West Asturian–Leonese and Central Iberian Zones of the Variscan Fold-Belt in NW Spain. *Geologische Rundschau* **81**(2), 545–560.

McClay, K. R. (1989) Analogue models of inversion tectonics. In *Inversion Tectonics*, eds M. A. Cooper and G. D. Williams, pp. 41–59. Geological Society of London Special Publication **44**.

McClay, K. R., Insley, M. W. and Anderton, R. (1989) Inversion of the Kechika Trough, Northeastern British Columbia, Canada. In *Inversion Tectonics*, eds M. A. Cooper and G. D. Williams, pp. 235–257. Geological Society of London Special Publication **44**.

McCulloch, D. S. (1989) Evolution of the offshore central California margin. In *The Eastern Pacific Ocean and Hawaii*, eds E. L. Winterer, D. M. Hussong and R. W. Decker, pp. 439–470. The Geology of North America, Vol. N. Geological Society of America.

McIntosh, K. D., Reed, D. L., Silver, E. A. and Meltzer, A. S. (1991) Deep structure and structural inversion along the central California continental margin from EDGE seismic profile RU-3. *Journal of Geophysical Research* **96**, 6459–6474.

Mitra, S. (1993) Geometry and kinematic evolution of inversion structures. *Bulletin of the American Association of Petroleum Geologists* **77**, 1159–1191.

Murata, K. J. and Larson, R. R. (1975) Diagenesis of Miocene siliceous shales, Temblor Range, California. *U.S. Geological Survey Journal of Research* **3**, 553–556.

Namson, J. and Davis, T. L. (1990) Late Cenozoic fold and thrust belt of the southern Coast Ranges and Santa Maria Basin, California. *Bulletin of the American Association of Petroleum Geologists* **74**, 467–492.

Narr, W. and Suppe, J. (1991) Joint spacing in sedimentary rocks. *Journal of Structural Geology* **13**, 1037–1048.

Nicholson, C., Sorlien, C. C. and Luyendyk, B. P. (1992) Deep crustal structure and tectonics in the offshore southern Santa Maria Basin, California. *Geology* **20**, 239–242.

Pisciotto, K. A. (1978) Basinal sedimentary facies and diagenetic aspects of the Monterey Shale, California. Unpublished Ph.D. thesis, University of California, Santa Cruz.

Pisciotto, K. A. and Garrison, R. E. (1981) Lithofacies and depositional environments of the Monterey Formation, California. In *The Monterey Formation and Related Siliceous Rocks of California*, eds R. E. Garrison, R. G. Douglas, K. A. Pisciotto, C. M. Isaacs and J. C. Ingle, pp. 97–122. Pacific Section of the Society of Economic Paleontologists and Mineralogists Special Publication **15**.

Ramsay, J. G. (1992) Some geometric problems of ramp–flat thrust models. In *Thrust Tectonics*, ed. K. R. McClay, pp. 191–200. Chapman and Hall, London.

Redwine, L. E. (1981) Hypothesis combining dilation, natural hydraulic fracturing and dolomitization to explain petroleum reservoirs in Monterey Shale, Santa Maria area, California. In *The Monterey Formation and Related Siliceous Rocks of California*, eds R. E. Garrison, R. G. Douglas, K. A. Pisciotto, C. M. Isaacs and J. C. Ingle, pp. 221–248. Pacific Section of the Society of Economic Paleontologists and Mineralogists Special Publication **15**.

Snyder, W. S., Brueckner, H. K. and Schweickert, R. A. (1983) Deformational styles in the Monterey Formation and other siliceous sedimentary rocks. In *Petroleum Generation and Occurrence in the Miocene Monterey Formation, California*, eds C. M. Isaacs and R. E. Garrison, pp. 151–170. Pacific Section of the Society of Economic Paleontologists and Mineralogists Special Publication **17**.

Snyder, W. S. (1987) Structure of the Monterey Formation: stratigraphic, diagenetic, and tectonic influences on style and timing. In *Cenozoic Basin Development of Coastal California—Rubey Volume VI*, eds R. V. Ingersoll and W. E. Ernst, pp. 321–347. Prentice-Hall, Englewood Cliffs, New Jersey.

Steinitz, G. (1981) Enigmatic chert structures in the Senonian cherts of Israel. *Bulletin of the Geological Survey of Israel* **75**, 1–46.

Steritz, J. W. and Luyendyk, B. P. (1994) Hosgri fault zone, offshore Santa Maria Basin, California. In *Seismotectonics of the Central California Coast Ranges*, eds I. B. Alterman, R. B. McMullen, L. S. Cluff and D. B. Slemmons. Geological Society of America Special Paper **292**.

Stock, J. (1992) A coupled diagenetic and micro-structural study of cherts from the Miocene Monterey Formation, California. Unpublished Senior thesis, University of California, Santa Cruz.

Sylvester, A. G. and Darrow, A. C. (1979) Structure and neotectonics of the western Santa Ynez fault system in southern California. *Tectonophysics* **52**, 389–405.

Vedder, J. G. (1987) Regional geology and petroleum potential of the southern California borderland. In *Geology and Resource Potential of the Continental Margin of Western North America and Adjacent Ocean Basins—Beaufort Sea to Baja California*, eds D. W. Scholl, A. Grantz and J. G. Vedder, pp. 403–447. Circum-Pacific Council for Energy and Mineral Resources **6**.

Vittori, E., Nitchman, S. P. and Slemmons, D. B. (1994) Stress pattern from late Pliocene and Quaternary brittle deformation in coastal Central California. In *Seismotectonics of Central California Coast Ranges*, eds I. B. Alterman, R. B. McMullen, L. S. Cluff and D. B.

Slemmons, pp. 31–43. Geological Society of America Special Paper **292**.

Williams, G. D., Powell, C. M. and Cooper, M. A. (1989) Geometry and kinematics of inversion tectonics. In *Inversion Tectonics*, eds M. A. Cooper and G. D. Williams, pp. 3–15. Geological Society of London Special Publication **44**.

Woodring, W. P. and Bramlette, M. N. (1950) *Geology and Paleontology of the Santa Maria District, California.* U.S. Geological Survey Professional Paper **222**.

Ziegler, P. A. (1983) Inverted basins in the Alpine foreland. In *Seismic Expression of Structural Styles—A Picture and Work Atlas*, ed. A. W. Bally, pp 3.3.3.–3.3.12. American Association of Petroleum Geologists, Studies in Geology, Series 15.